DOI: 10.1002/ejic.201000734

Synthesis and Characterization of Colloidal Core–Shell Semiconductor Nanowires

Zhen Li,*[a,b] Xuedan Ma,[a] Qiao Sun,[c] Zhe Wang,[a] Jian Liu,[b] Zhonghua Zhu,[d] Shi Zhang Qiao,[b] Sean C. Smith,[c] Gaoqing (Max) Lu,*[b] and Alf Mews*[a]

Keywords: Nanotechnology / Nanostructures / Semiconductors / Cadmium / Core–shell structures

CdSe colloidal nanowires, generated from solution-liquid-solid approach, have been coated with CdS rods (or ribbons) by using cadmium hexadecyl xanthate (Cd-HDX) as a single source precursor. The use of different solvents and ligands causes pronounced effects on the morphology of the nanowires. The coating process includes nucleation and growth of CdS nanorods onto the core CdSe nanowires, followed by ripening of the CdS nanorods to produce the desired core-shell nanowire structure.

Introduction

During the past decades, cadmium selenide (CdSe) nanostructures such as dots, rods and wires have been extensively investigated due to their unique properties (e.g., quantum confinement effects) and potential applications in bioimaging, solar cells, light-emitting diodes and other nanodevices.[1,2] Compared with quantum dots and rods, CdSe nanowires are particularly important because they can be easily contacted by standard lithographic techniques. CdSe nanowires are traditionally prepared by nonwet chemical methods such as the vapor–liquid–solid (VLS) technique,[3] the laser-catalyst growth (LCG) approach[4] or the thermal evaporation of bulk material.[5] However, most nanowires are beyond the quantization regime and the lack of dispersibility limits their applications. Recently, the focus of synthesis has shifted toward colloidal quantum nanowires prepared by using wet-chemical methods. One versatile solution approach is the solution–liquid–solid (SLS) method, which uses low-melting-point nanoparticles as nanoreactors for the nucleation and growth of nanowires to tune the nanowire diameter over a wide range.[6,7] This method has also been extended to the preparation of blocked heteronanowires and doped nanowires.[8–11]

Compared with quantum dots and rods, photogenerated charge carriers or excitons in one-dimensional nanowires can diffuse along the wire and interact with a larger surface area. This increases the interaction with surface trap states, which is the most probable reason for the reduced luminescence of nanowires. These surface traps might originate from the surface ligands, which can possibly serve as charge donors or acceptors. Therefore photogenerated electrons or holes can be transferred to the surface ligands, thereby quenching the luminescence of the nanowires. In addition, the surface ligands can be chemically degraded and detached from the surface, thus reducing the photochemical stability of nanowires. To improve the luminescence and photo stability of the CdSe core, wide-band-gap shells of cadmium sulfide (CdS) and zinc sulfide (ZnS) have been coated onto the surface to eliminate surface defects, which has been demonstrated in the cases of quantum dots and rods.[12,13]

There are several approaches for the preparation of core–shell nanostructures by wet-chemical methods. The first one uses highly reactive agents such as dimethyl cadmium ($CdMe_2$), diethylzinc ($ZnEt_2$) and hexamethyldisilathiane [$(TMS)_2S$] as cationic and anionic precursors, respectively.[13,14] Although core–shell quantum dots and rods can be synthesized by this method, it is difficult to eliminate the homogeneous nucleation of shell materials and ensure a homogeneous shell around each core. Therefore, Peng et al. have developed a successive ion-layer adsorption and reaction (SILAR) technique to epitaxially grow shells in a noncoordinating solvent.[15] The precursors used are less reactive so as to prevent independent nucleation of the shell material, but still sufficiently reactive to promote epitaxial

[a] Institute of Physical Chemistry, The University of Hamburg
Grindelallee 117, 20146 Hamburg, Germany
Fax: +49-40-428387727
E-mail: mews@chemie.uni-hamburg.de
[b] ARC Centre of Excellence for Functional Nanomaterials, Australian Institute for Bioengineering and Nanotechnology, The University of Queensland, QLD 4072, Australia
Fax: +61-7-33463973
E-mail: z.li3@uq.edu.au
maxlu@uq.edu.au
[c] Centre for Computational Molecular Science, Australian Institute for Bioengineering and Nanotechnology, The University of Queensland, QLD 4072, Australia
Fax: +61-7-33463973
[d] The Department of Chemical Engineering, The University of Queensland, QLD 4072, Australia

Supporting information for this article is available on the WWW under http://dx.doi.org/10.1002/ejic.201000734.

growth of the shell around the existing cores. By using this technique, robust core–shell nanocrystals with a quantum yield more than 80% can be synthesized.[12,15] It should be noted that the SILAR method is not applicable for preparing core–shell nanorods due to the thermal instability of nanorods, which start to shrink above 160 °C.[13] A seed-mediated growth method has also been established in which, for example, CdSe@CdS nanorods can be prepared by mixing CdSe nanocrystals with a sulfur precursor solution [TOPS, prepared by dissolving sulfur in trioctylphosphane (TOP)] and then injected into a Cd precursor solution.[16] The CdSe nanoseeds are embedded on one side of the CdS rods. These asymmetric CdSe@CdS nanorods show a higher fluorescence quantum yield (QY) than the symmetric core–shell nanorods prepared from epitaxial growth, which is attributed to the natural difference between initial dot and rod cores.

Despite advancements in the synthesis of core–shell colloidal nanodots and -rods, there are only a few reports on core–shell colloidal nanowires. Recently Kuno et al. prepared core–shell nanowire heterostructures by using highly reactive $CdMe_2$, $ZnEt_2$ and $(TMS)_2S$ as precursors at high temperature (250 °C).[17] Their results show that the core–shell wires display a suppression of Auger processes, but a significant quenching of the wire fluorescence (QY < 0.05% for CdSe@CdS nanowires). In addition, the photochemical stability of these nanowires is unknown. Therefore, it remains a significant challenge to develop a novel method for the preparation of robust core–shell nanowires with high fluorescence QY. Here we adopt a stable single precursor for Cd and S to coat CdSe nanowires at low reaction temperature (<130 °C). The decomposition of the single source precursor leads to the formation of nanorods on the surface of the nanowires, thereby resulting in brushlike nanowires that gradually transform into core–shell structures through a ripening process. We show that this coating method does not lead to a reduction of the fluorescence intensity but rather to a higher fluorescence QY than the uncoated parent nanowires.

Results and Discussion

Synthesis and Characterization of Core–Shell Nanowires

As mentioned already, high-quality colloidal CdSe nanowires have been achieved by the solution–liquid–solid (SLS) approach.[18–21] Also, the formation of core–shell nanowires in a noncoordinating solvent, octadecene (ODE), by using highly reactive $CdMe_2$, $ZnEt_2$ and $(TMS)_2S$ as precursors at 250 °C has been performed by Kuno et al.[17] Hence, we initially used the same cationic and anionic precursors to prepare core–shell nanowires in a coordinating solvent, trioctylphosphane oxide (TOPO), which has also been extensively applied to core–shell nanorods.[13,14] Our nanowires were modified with 1-hexadecylamine (HDA) through ligand-exchange processes, which does not degrade the nanowires, as proved by their similar diameters (see part a of Figure 1 and Figure S1 in the Supporting Information). We found that parent CdSe nanowires are not stable after dropwise addition of the highly reactive precursor solutions at 140 °C. In particular, when the reaction temperature was increased to 245 °C, the resulting core–shell nanorods were considerably shorter than those of the parent CdSe nanowires, as shown in part b of Figure 1, and wires with a length of only several hundred nanometers were generated. However, the diameter of the nanowires increases from 11 to 22 nm after coating, as expected (Figure S2 in the Supporting Information).

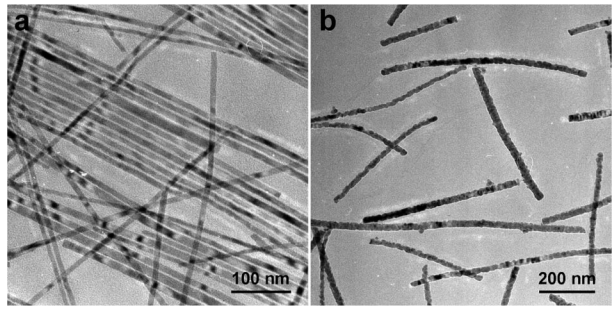

Figure 1. TEM images of (a) CdSe nanowire cores and (b) core–shell CdSe@CdS/ZnS nanowires obtained from highly reactive precursors.

To establish the effects of different solvents on the thermal stability of CdSe nanowires, we cooked nanowires in several solvents including TOPO, TOP, ODE and oleylamine (OLA) for 90 min. The results show that these nanowires are unstable in all investigated solvents at high temperature (>200 °C), but stable at low temperature (<120 °C), except for OLA, which can decompose CdSe nanowires completely after 60 min.

The thermal instability of the nanowires encouraged us to look for moderate precursors to coat nanowires at low temperature (<160 °C). Here we chose cadmium hexadecyl xanthate (Cd-HDX) as a precursor since it can be decomposed at different temperatures, depending on the specific solvents used.[22] Figure S3 in the Supporting Information shows the absorption evolution of Cd-HDX in different solvents at different temperatures. If TOP is used as a solvent (Figure S3a), the characteristic absorption of Cd-HDX at 300 nm decreases most strongly if the temperature exceeds 90 °C. The replacement of TOP with HDA leads to the complete decomposition of the Cd-HDX precursor even below 70 °C, which is indicated by the disappearance of the absorption peak at 300 nm (Figure S3b). In addition, a new absorption peak attributed to CdS nanoparticles appears at 363 nm, even at 50 °C. Using liquid oleylamine as solvent resulted in the formation of CdS nanoparticles even at room temperature upon overnight stirring (Figure S3c). These findings suggest that Lewis bases such as alkylamines can significantly reduce the decomposition temperature. The decomposition of the Cd-HDX precursor probably proceeds through a β-elimination mechanism as in the Chugaev reaction.[22] Since our nanowires are more stable in TOP than in pure OLA, we chose TOP as solvent for the preparation of core–shell nanowires.

Figure 2 shows the TEM images of nanowires obtained at different stages of the nanowire coating process. The core nanowires exhibit a smooth surface and their diameter is (33 ± 7.0) nm (Figure 2, a). After growth of a calculated amount of 6 monolayers of CdS (see the Experimental Section for calculations) from Cd-HDX in TOP at 90 °C, the nanowire diameter is retained at (33 ± 8.5) nm but there are some nanorods formed on the surface (Figure 2, b). These bristlelike nanorods are (2.1 ± 0.4) nm in diameter and (6.0 ± 1.1) nm in length. Further addition of precursor solution leads to an increase of nanorod size. After growth of calculated 10 monolayers of CdS, the reaction mixture was heated to 130 °C. The final diameter and length of the nanobristles was respectively increased to (3.6 ± 0.6) and (10.4 ± 1.8) nm after reaction for 2 h (Figure 2, c), accompanied by a slight increase in the nanowire "core" diameter [(35 ± 5.5) nm]. Prolonging the reaction time to 14 h leads to the disappearance of some of the nanobristles but the diameter of the remaining nanorods is increased to (6.2 ± 0.91) nm and their length is shrunk to (8.3 ± 1.9) nm (Figure 2, d). Meanwhile, the average diameter of nanowires is further increased to 36 nm.

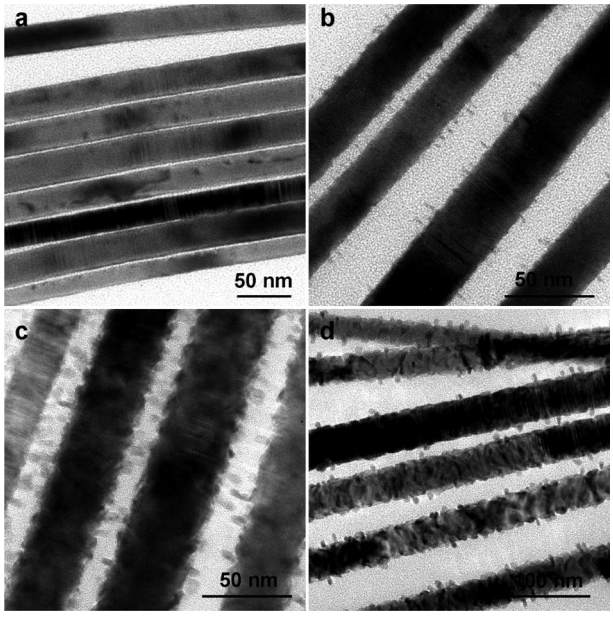

Figure 2. TEM images of (a) the parent CdSe nanowire and (b–d) core–shell CdSe@CdS nanowires obtained at different stages by using Cd-HDX as precursor.

The resulting nanowires were further characterized with high-resolution TEM (HRTEM; Figure 3, a). The shell is labelled with arrows, and the shell thickness is around 4 nm. In addition to the interface between core and shell, different interfaces between the shell and "attached islands", probably attached nanorods or nanoparticles, are also observed. Compared with the parent nanowires, it is more difficult to distinguish the interface between wurtzite (W) and zincblende (ZB) fractions of the wire core by HRTEM after coating.[20,23] The composition of the core–shell nanowires was determined by energy-dispersive X-ray spectroscopy (EDX; Figure S4 in the Supporting Information). The results clearly reveal the presence of Cd, Se and S, as expected, and their atomic percentage is 46, 41 and 13%, respectively.

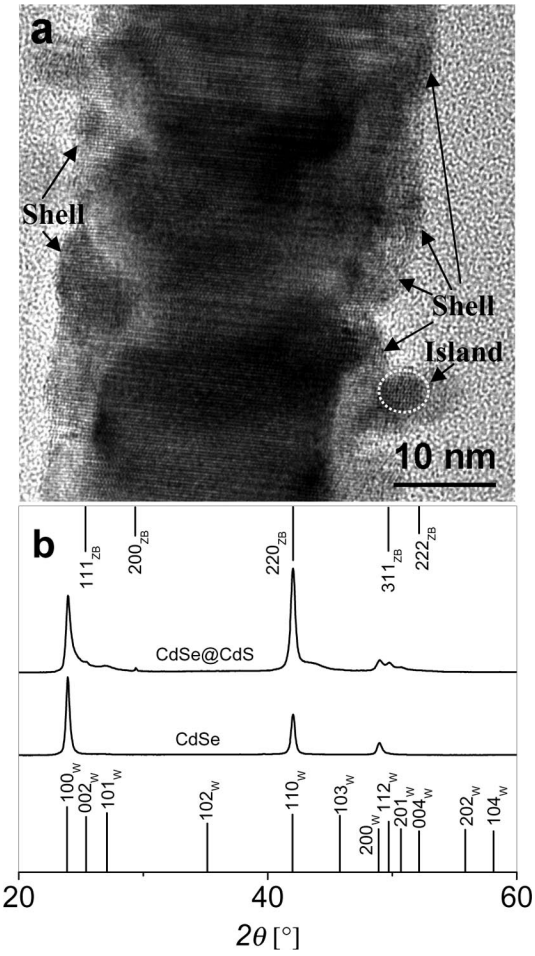

Figure 3. (a) HRTEM image of core–shell CdSe@CdS nanowires and (b) XRD patterns of the parent and core–shell nanowires. The top and bottom sticks are the standard patterns of zincblende and wurtzite CdSe.

The core–shell nanowires were also investigated by powder X-ray diffraction (XRD; Figure 3, b). Compared to the standard diffraction pattern of bulk W and ZB phases, the intensity ratios among the indexed peaks of parent and core–shell nanowires are quite different, which is likely caused by depression and enhancement of diffraction peaks induced by the sample geometry.[19] In general, in X-ray diffraction only crystallographic layers that lie perpendicular to the angle bisector of the incident and reflected beam show strong reflections. Since we used Bragg–Brentano geometry in which the nanowires lie completely flat on the substrate, only the planes that lie parallel to the substrate surface, and hence parallel to the nanowire length axis, would show strong reflections. Thus, for W nanowires that grew along the [001] direction, only the (100), (110) and (200) peaks in Figure 3 (b) show strong diffraction intensity.

In contrast, for the CdSe@CdS nanowires, the attached nanorods are not necessarily aligned in this way and some additional peaks are visible in their XRD patterns.

Formation Mechanism of Core–Shell Nanowires

Due to the inhomogeneous crystal structure of the nanowire (i.e., admixture of wurtzite and zincblende), pronounced growth defects and the large surface area, the formation mechanism of core–shell nanowires is very complicated. On the basis of the above results, there are most likely two processes involved in the formation of core–shell CdSe@CdS nanowires (Scheme 1). The first one is the nucleation and growth of CdS nanorods on the surface of CdSe nanowires, which is governed by the amount of precursor (i.e., monomer concentration) of the shell material, possible surface defects of the core nanowires and the ligands used.[24] If a low-concentration precursor solution (0.05 M) is added stepwise, this significantly reduces self-nucleation of nanorods in the solution. The growth of nanorods onto the surface of the nanowires might then be mediated by different surface facets or defects, which provide active sites for the nucleation. Therefore, CdS can nucleate on the nanowire surface and then grow into nanorods upon continuous supply of Cd-HDX precursor.

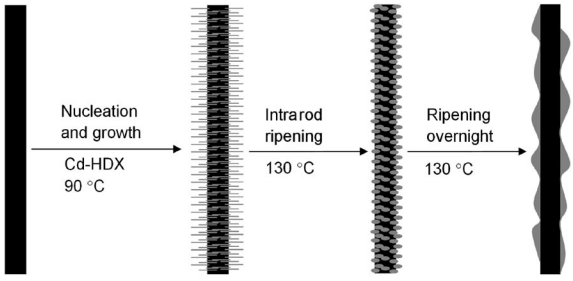

Scheme 1. Coating CdSe nanowires with CdS shell from a single Cd-HDX precursor.

The nucleation and growth of nanorods is also influenced by the ligands because of their different affinities to the various facets of crystals. Basically, the XRD patterns of the CdSe@CdS nanowires suggest that CdS nanorods grow predominantly in the W phase. For isolated W nanorods it has been shown that they grow along the (001) axis.[25] In addition, the (001) facets at the ends of the rods can be either terminated with Cd or S atoms such that there is a permanent dipole along this *c* axis. For the CdSe nanowires it has been shown that they consist of sections of W and ZB. Hence it might well be that the CdS rods nucleate predominantly to the ZB surface sites of the nanowires, similar to the growth of tetrapods.[26] For this mechanism to happen, the affinities of ligands to the respective surface sites should play a key role in the growth of nanorods.[27] Figure 4 (a–c) shows the TEM images of brushlike nanowires obtained from different solvents and/or ligands. When TOP is used as both solvent and ligand, most nanowires are not coated but the CdS nanorods are only adsorbed onto the nanowire surface (Figure 4, a). Moreover, large quantities of free CdS nanoparticles have been generated in solution. Adding one-fifth OLA (volume ratio) into the TOP solution leads to the formation of more uniform thinner and longer nanorods directly on the surface of the parent nanowires, with a diameter of (2.9 ± 0.5) nm and a length of (11.2 ± 2.6) nm (Figure 4, b). A typical HRTEM image is shown in Figure 5 (a). It can be seen that most bristles take a similar crystal orientation to the core and only a few of them are oriented in a different way (i.e., they are mainly a wurtzite structure), which is consistent with XRD results (Figure 3, b) and supports the nucleation and growth of nanorods on the surface of nanowires.

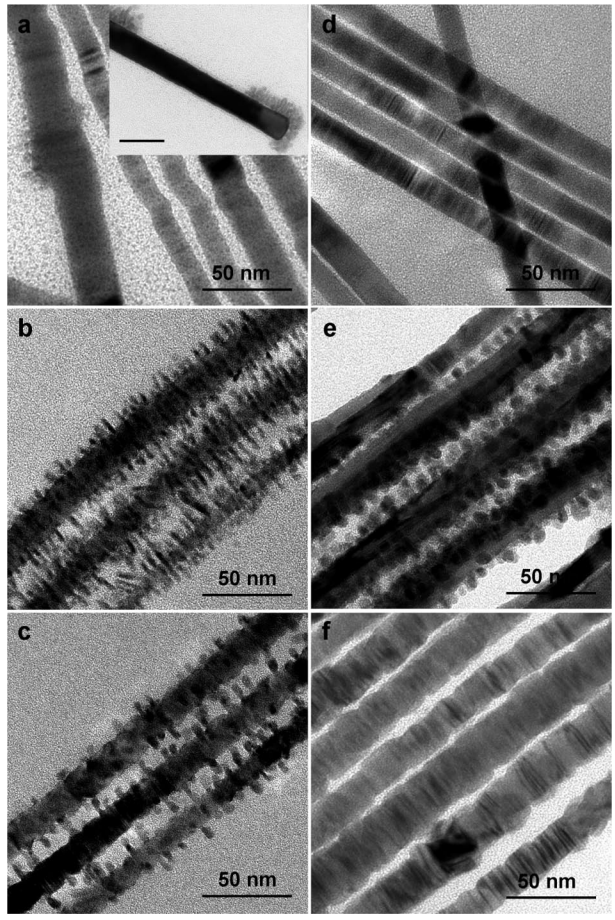

Figure 4. TEM images of core–shell CdSe@CdS nanowires prepared in (a) pure TOP, (b) a mixture of TOP and OLA and (c) a mixture of TOP, OA and OLA. Image (d) is the original CdSe nanowires and (e–f) are core–shell CdSe@CdS nanowires ripened for 4 and 24 h.

Using a mixture of TOP, OLA and OA in a volume ratio of 5:1:1 produces similar distributed nanorods with a thicker diameter [(5.1 ± 0.7) nm] and shorter length [(7.7 ± 1.6) nm]. These results suggest that the role of OLA and OA in the growth of nanorods is contrary (i.e., OLA promotes longitudinal growth, and OA favours transverse growth). Such a difference can be explained in a first approximation from viewpoints of elemental electronegativ-

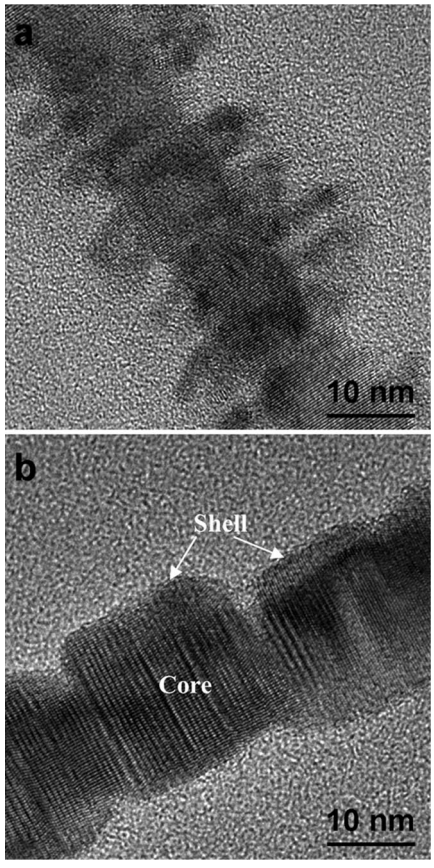

Figure 5. HRTEM images of CdSe@CdS nanowires shown in Figure 4 (see parts b and f).

ities. The order of ligand affinity to Cd atoms is TOP < OLA < OA because the electronegativity of elements P, N and O is 2.2, 3.0 and 3.4, respectively.[28]

The second process is the intrarod ripening, which is a thermodynamically driven process.[29] In principle, one-dimensional nanostructures such as nanorods will eventually evolve to the most stable zero-dimensional dot shape if the growth process is diffusion-controlled and no additional precursor is added to the reaction solution.[24] In this mechanism, "surface CdS" can be transferred in an intrarod manner,[24] thereby converting rods into dot shapes as proved by the increase in the diameter of the rods and the decrease in their length. In our experiments, the CdS rods are attached to the CdSe wires and "CdS units" can also diffuse along the CdSe nanowires due to their favourable wetting and small lattice mismatch between CdSe and CdS (3.9%). The overall result of this ripening process is the disappearance of CdS nanorods and the formation of CdS ribbons on the surface. To further prove this ripening process, we repeated the coating process and prolonged ripening time. Figure 4 (d–f) shows the TEM images of parent CdSe nanowires and core–shell nanowires after ripening for 4 and 24 h. Compared with parent nanowires, there are many CdS nanodots attached to the surface of the nanowires after 4 h of ripening (Figure 4, e). One typical single-wire image is shown in Figure S5 of the Supporting Information. After ripening for 24 h, these CdS dots are completely converted into ribbons along nanowires (Figure 4, f). The typical HRTEM image is presented in Figure 5 (b); it clearly demonstrates the core–shell structure. Furthermore, the shell and core are orientated in the same crystal phase, which suggests the diffusion of CdS units along the wire.

It should be noted that when the same conditions were applied to coat CdSe nanowires from a Zn-HDX single precursor, isolated thin and long ZnS nanorods were formed that are not attached to the CdSe parent nanowires (Figure S6 in the Supporting Information). Hence, after thermal ripening and purification, the resulting nanowires were purely CdSe as proved by EDX. The failure of this material combination to coat is attributed to the large lattice mismatch between CdSe and ZnS (12%). Hence, the coating of nanowires is much more complicated than the coating of nanodots, and the coating conditions will certainly be the subject of further investigations.

Optical Properties and Stability of Core–Shell Nanowires

One important motivation for the synthesis of core–shell nanowires is the modification, and ideally manipulation, of optical and electronic properties. In general, different types of core–shell nanostructures can either lead to an effective confinement or separation of photogenerated charge carriers within the core and shell. According to their electronic structures, our CdSe@CdS nanowires belong to a type-I structure in which the conduction band and valence band of the shell material are respectively higher and lower than that of the core material. The energy difference between their conduction bands of the respective bulk materials is only 0.2 eV so that the photogenerated electrons can easily delocalize over the whole core–shell structure.[13] This results in a slight redshift of the absorption and emission spectra upon coating, especially when thin core wires are used.

Due to the weak fluorescence of nanowires, it is difficult to determine their photoluminescence (PL) and quantum yield (QY) by comparison with a standard dye solution with a high-fluorescence QY. Hence we used a two-step process by first determining the QY of semiconductor nanocrystals (NCs) that emit in a similar wavelength range to the nanowires to be 10%, relative to the standard dye (rhodamine 6G). Then in a second step we compared the PL intensity of the wires with those of the NCs by using a microscope setup with a sensitive CCD camera. The NCs used were CdTe@ZnSe/ZnSeS/ZnS particles that had been prepared within the scope of another project. A typical TEM image of those reference quantum dots as well as UV/Vis and PL spectra of the dye and reference NCs are shown in Figure S7 in the Supporting Information.

Figure 6 shows the UV/Vis and photoluminescence spectra of parent CdSe nanowires (Figure 4, d) and CdSe@CdS nanowires obtained at different reaction stages. Since the diameter of the parent CdSe nanowires was already

(17.4 ± 4.0) nm, there is no redshift after coating but the absorption edge becomes less steep. Hence, only the additional absorption peak at 480 nm can be associated to the presence of CdS, which can be better seen from the second derivative of the spectra shown in Figure S8 of the Supporting Information. The photoluminescence of nanowires was recorded upon excitation with a 470 nm laser. Here we observed a similar emission centred at 704 nm for both parent and core–shell nanowires. The similar emission wavelength, together with similar absorption, demonstrate that the nanowires are already beyond the strong confinement regime [i.e., their diameter is larger than the bulk exciton dimensions (ca. 11 nm)]. However, the shell material influences the fluorescence QY of the nanowires. The QY of the parent nanowires is 0.14% and is not strongly influenced by coating with calculated two monolayers of CdS. After further increasing the shell thickness to 6 and 10 monolayers, the QYs increased respectively to 0.25 and 0.46%. However, ripening the core–shell nanowires in an overnight reaction at 130 °C again decreased the QY to 0.20%. This trend is similar to core–shell CdSe@CdS nanodots and rods (i.e., the QYs increase first upon shell growth and then decline upon ripening).[13] However, the results show that the fluorescence quantum yield can be improved by at least a factor of 2–3.

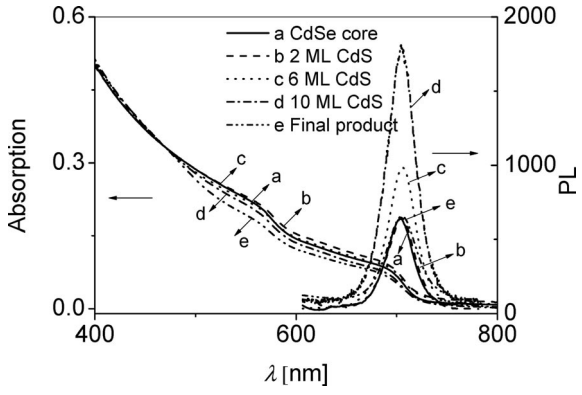

Figure 6. UV/Vis absorption and photoluminescence spectra of parent and core–shell CdSe@CdS nanowires.

Conclusion

Colloidal semiconductor CdSe nanowires, generated by a solution–liquid–solid (SLS) approach, have been successfully coated with a CdS shell from the single-source precursor Cd-HDX at low temperature, thus resulting in core–shell nanostructures. The coating process consists of nucleation and growth of CdS nanorods on the CdSe nanowire surface, followed by ripening of the nanorods to form CdS ribbons. The CdS shell does not alter the characteristic absorption and emission of the CdSe core, but changes the quantum yield of the parent nanowires.

Experimental Section

Materials: Cadmium oxide (CdO, 99.99%), selenium powder (Se, 99%), 1-hexadecylamine (HDA, 98%), octanoic acid (99%), oleic acid (OA, 70%), oleylamine (OLA, 70%), octyl ether (99%), diethylzinc ($ZnEt_2$) and hexamethyldisilathiane [$(TMS)_2S$] were purchased from Aldrich. Trioctylphosphane oxide (TOPO, 98%) and trioctylphosphane (TOP, 90%) were received from Merck and Fluka, respectively. Dimethyl cadmium ($CdMe_2$) was used as received (Strem Chemicals). TOPSe stock solutions (2.0 M) were prepared by dissolving Se (1.60 g) into TOP (10.0 mL) with shaking under air-free conditions. Bismuth (Bi) nanocatalysts were prepared from the reduction of bismuth chloride ($BiCl_3$, 99.99%, Acros) or $Bi[N(SiMe_3)_2]_3$ with TOP at room temperature.[20,30] Metal hexadecyl xanthates (Cd-HDX and Zn-HDX) were synthesized according to previous reports.[22] Stock solution (0.05 M) was prepared by dissolving Cd-HDX (186.4 mg) in TOP (4.8 mL).

Preparation of Parent CdSe Nanowires: CdSe nanowires were prepared as described elsewhere.[20] A mixture of CdO, TOPO and octanoic acid was loaded into a 50 mL three-necked flask. This mixture was dried and degassed for 30 min at 100 °C under vacuum (1 mbar). Then the flask was backfilled with Ar. The temperature was increased to completely dissolve CdO and then decreased to the desired temperature. Afterwards, a mixture of Bi nanoparticles and TOPSe was injected. The solution was kept at the reaction temperature for a certain time before cooling. When the temperature was decreased to 80 °C, toluene (2–4 mL) was added to the solution to prevent the TOPO from solidifying. The resulting nanowires were separated from the mixture by using high-speed centrifugation (18000 rpm, 10 min). The obtained nanowires were washed with toluene for several times and finally dispersed in chloroform. The nanowire diameter and length can be tailored to suit a wide range of desired measurements by controlling the competition among the growth of nanocatalysts, the growth of nanowires and the growth of nanocrystals.

Surface Ligand Exchange: The as-synthesized CdSe nanowires and HDA (0.50 g) were dissolved in $CHCl_3$ (30 mL) and then stirred overnight at 50 °C. Afterwards, CdSe nanowires were separated by high-speed centrifugation and redissolved in $CHCl_3$ as stock solution. For convenience, these nanowires are called HDA-capped CdSe nanowires. The ligand exchange improved the dispersbility of nanowires in common organic solvents such as chloroform and toluene without degradation.

Synthesis of Core–Shell Nanowires by Using $CdMe_2$, $ZnEt_2$ and $(TMS)_2S$ as Precursors: TOPO (1.01 g) was loaded into a 50 mL three-necked flask and dried for 30 min at 100 °C. After the flask was backfilled with Ar, HDA-capped CdSe nanowire $CHCl_3$ solution (0.4 mL) was added (A_{674} = 0.071); the calculated concentration is around 3.9×10^{-10} M by using 1.81×10^8 as the molar excitation coefficient of CdSe nanowires at the band edge[31]). The solvent was removed under vacuum using a pump, and the solution temperature was increased to 140 °C. Then a solution of $CdMe_2$ (0.15 mmol) and $(TMS)_2S$ (0.31 mmol, 55.0 mg) in TOP (0.4 mL) was added dropwise into the nanowire solution, followed by a solution of $ZnEt_2$ (0.15 mmol) in TOP solution (0.2 mL). After addition, the temperature was increased to 245 °C and the reaction continued for 10 min. Then the temperature was decreased to 80 °C and toluene (2 mL) was added into the mixture. The resulting core–shell nanowires were separated by high-speed centrifugation (18000 rpm, 10 min) and washed several times with toluene. The final product was dissolved in $CHCl_3$ and used for characterization.

Calculations of the Amount of Precursor Solutions for Shell Growth: The calculations of growth of core–shell nanowires are similar to the growth of core–shell nanocrystals by using the SILAR method. The concentration of CdSe nanowire cores (c) can be estimated from Equation (1).

$$A = \varepsilon c \quad (1)$$

in which A is the absorption value and ε is the molar extinction coefficient of CdSe nanowires (i.e., 1.81×10^8 to 1.02×10^{10} M^{-1} cm^{-1} for nanowires with a diameter of 6 to 42 nm at the band edge, and 8.84×10^8 to 1.44×10^{10} M^{-1} cm^{-1} at 488 nm).[31] The amount of the injection solution (V) for each monolayer can be deduced on the basis of a cylinder model from Equation (2).

$$\Delta V = \pi L[2Rd + (2n - 1)d^2] \quad (2)$$

in which R and L are the diameter and length of nanowires, respectively. In this manuscript, the average diameter of nanowires used is 10, 17 and 33 nm, respectively, and their average length is between 10 and 6 μm. The value d is the thickness of a monolayer of CdS (0.35 nm).

Synthesis of Core–Shell Nanowires Using M-HDX as Precursors: A mixture of TOP (5 mL), oleic acid (OA; 1 mL) and oleylamine (OLA; 1 mL) was added into a 50 mL three-necked flask, then CdSe nanowire $CHCl_3$ solution (2.0 mL) was added (A_{700} = 0.103); the calculated concentration is around 5.7×10^{-10} M). The $CHCl_3$ was pumped off and the solution was dried at 50 °C for 60 min. Then the mixture was heated to 90 °C under the protection of argon and a calculated amount of Cd-HDX precursor solution (0.05 M) for growing the first monolayer was injected. The solution was allowed to react for 30 min before the injection of precursor solution for the second layer. After growing the desired thickness of shell, the reaction mixture was heated to 130 °C and the reaction continued overnight. The purification of nanowires is similar to previous parent nanowires.

Characterizations: Low-resolution TEM images were recorded with a JEOL 1011 electron microscope operating at an acceleration voltage of 100 kV. HRTEM images and EDX were collected with a Philips CM 300 UT microscope operating at an acceleration voltage of 200 kV. TEM samples were prepared by dropping a diluted solution of nanowires in $CHCl_3$ onto carbon-coated copper grids. The nanowire crystal structure was determined by X-ray diffraction performed with a Philipps X′Pert diffractometer. UV/Vis spectra were measured with a Cary 50 UV/Vis spectrometer. The fluorescence of nanowire solutions was investigated with a confocal microscope with 470 nm laser as the excitation source. The fluorescent CdTe@ZnSe/ZnSeS/ZnS quantum dots with an emission of 723 nm were used as a reference to determine the nanowire quantum yield.

Supporting Information (see also the footnote on the first page of this article): Nanowire diameter distribution, UV/Vis absorption of precursor, TEM images and EDX of nanowires.

Acknowledgments

The authors thank Mrs. Sylvia Bartholdi-Nawrath and Mrs. Almut Barck for the HRTEM characterization and XRD measurements. The authors also thank Ms. Jessica Völker for providing QDs. Z. L. gratefully acknowledges financial support by 2008004276 (Queensland Smart Future Fellowship), 2009000238 (Queensland International Fellowship), 2009002539 (The University of Queensland (UQ) ECR grant) and 2009003505 (UQ New Staff Funding). The work was funded by the Deutsche Forschungsgemeinschaft (DFG) (ME 1380/16-1).

[1] X. Michalet, F. F. Pinaud, L. A. Bentolila, J. M. Tsay, S. Doose, J. J. Li, G. Sundaresan, A. M. Wu, S. S. Gambhir, S. Weiss, *Science* **2005**, *307*, 538–544.
[2] W. U. Huynh, J. J. Dittmer, A. P. Alivisatos, *Science* **2002**, *295*, 2425–2427.
[3] R. S. Wagner, W. C. Ellis, *Appl. Phys. Lett.* **1964**, *4*, 89–90.
[4] X. F. Duan, C. M. Lieber, *Adv. Mater.* **2000**, *12*, 298–302.
[5] C. Ma, Z. L. Wang, *Adv. Mater.* **2005**, *17*, 2635–2639.
[6] F. D. Wang, A. G. Dong, J. W. Sun, R. Tang, H. Yu, W. E. Buhro, *Inorg. Chem.* **2006**, *45*, 7511–7521.
[7] M. Kuno, *Phys. Chem. Chem. Phys.* **2008**, *10*, 620–639.
[8] L. Ouyang, K. N. Maher, C. L. Yu, J. McCarty, H. Park, *J. Am. Chem. Soc.* **2007**, *129*, 133–138.
[9] A. G. Dong, F. D. Wang, T. L. Daulton, W. E. Buhro, *Nano Lett.* **2007**, *7*, 1308–1313.
[10] N. Fu, Z. Li, A. Myalitsin, M. Scolari, R. T. Weitz, M. Burghard, A. Mews, *Small* **2010**, *6*, 376–380.
[11] Z. Li, L. N. Cheng, Q. Sun, Z. H. Zhu, M. J. Riley, M. Aljada, Z. X. Cheng, X. L. Wang, G. R. Hanson, S. Z. Qiao, S. C. Smith, G. Q. Lu, *Angew. Chem. Int. Ed.* **2010**, *49*, 2777–2781.
[12] R. G. Xie, U. Kolb, J. X. Li, T. Basche, A. Mews, *J. Am. Chem. Soc.* **2005**, *127*, 7480–7488.
[13] L. Manna, E. C. Scher, L. S. Li, A. P. Alivisatos, *J. Am. Chem. Soc.* **2002**, *124*, 7136–7145.
[14] X. G. Peng, M. C. Schlamp, A. V. Kadavanich, A. P. Alivisatos, *J. Am. Chem. Soc.* **1997**, *119*, 7019–7029.
[15] J. J. Li, Y. A. Wang, W. Z. Guo, J. C. Keay, T. D. Mishima, M. B. Johnson, X. G. Peng, *J. Am. Chem. Soc.* **2003**, *125*, 12567–12575.
[16] L. Carbone, C. Nobile, M. De Giorgi, F. D. Sala, G. Morello, P. Pompa, M. Hytch, E. Snoeck, A. Fiore, I. R. Franchini, M. Nadasan, A. F. Silvestre, L. Chiodo, S. Kudera, R. Cingolani, R. Krahne, L. Manna, *Nano Lett.* **2007**, *7*, 2942–2950.
[17] J. A. Goebl, R. W. Black, J. Puthussery, J. Giblin, T. H. Kosel, M. Kuno, *J. Am. Chem. Soc.* **2008**, *130*, 14822–14833.
[18] H. Yu, J. B. Li, R. A. Loomis, P. C. Gibbons, L. W. Wang, W. E. Buhro, *J. Am. Chem. Soc.* **2003**, *125*, 16168–16169.
[19] J. W. Grebinski, K. L. Hull, J. Zhang, T. H. Kosel, M. Kuno, *Chem. Mater.* **2004**, *16*, 5260–5272.
[20] Z. Li, Ö. Kurtulus, F. Nan, A. Myalitsin, Z. Wang, A. Kornowski, U. Pietsch, A. Mews, *Adv. Funct. Mater.* **2009**, *19*, 3650–3661.
[21] F. D. Wang, W. E. Buhro, *Small* **2010**, *6*, 573–581.
[22] N. Pradhan, B. Katz, S. Efrima, *J. Phys. Chem. B* **2003**, *107*, 13843–13854.
[23] Ö. Kurtulus, Z. Li, A. Mews, U. Pietsch, *Phys. Stat. Sol. A* **2009**, *206*, 1752–1756.
[24] X. G. Peng, *Adv. Mater.* **2003**, *15*, 459–463.
[25] Z. A. Peng, X. G. Peng, *J. Am. Chem. Soc.* **2001**, *123*, 1389–1395.
[26] L. Manna, E. C. Scher, A. P. Alivisatos, *J. Am. Chem. Soc.* **2000**, *122*, 12700–12706.
[27] Z. A. Peng, X. G. Peng, *J. Am. Chem. Soc.* **2002**, *124*, 3343–3353.
[28] L. Pauling, *J. Am. Chem. Soc.* **1932**, *54*, 3570–3582.
[29] L. Ratke, P. W. Voorhees, in: *Growth and Coarsening - Ostwald Ripening in Material Processing* (Eds.: L. Ratke, P. W. Voorhees), Springer, **2002**, pp. 117–118.
[30] Z. Li, A. Kornowski, A. Myalitsin, A. Mews, *Small* **2008**, *4*, 1698–1702.
[31] V. Protasenko, D. Bacinello, M. Kuno, *J. Phys. Chem. B* **2006**, *110*, 25322–25331.

Received: July 5, 2010
Published Online: August 24, 2010

